43rd AIAA/ASME/SAE/ASEE Joint Propulsion Conference & Exhibit
8 - 11 July 2007, Cincinnati, OH

AIAA 2007-5220

Preliminary Results of a High Frequency Pulsed Plasma Thruster

R. I. Marques[1,2] , S. B. Gabriel[1], F. de S. Costa[2].
[1] *Astronautics Research Group*
University of Southampton
United Kingdom

[2] *INPE -Instituto Nacional de Pesquisas Espaciais*
LCP -Laboratório de Combustão e Propulsão
Cachoeira Paulista – SP, Brazil

ABSTRACT

Pulsed Plasma Thrusters (PPTs) are long standing electric propulsion thrusters that are reliable, relatively simple and low cost. One of the main issues with PPTs is its low efficiency (discharge energy vs. exhaust jet's kinetic energy), typically between 3-8%. One of the main contributors for the low performance in PPTs is the late time ablation (LTA). LTA is the sublimation of propellant that takes place after the main discharge, due to the propellant, usually Teflon®, temperature being above its sublimation point. The LTA produces a low speed gas and macro particles that does not contribute significantly to produce thrust. The High Frequency Pulsed Plasma Thruster (HFB-PPT) is a novel patented design that aims at accelerating the late time ablation by employing additional discharges after the main discharge. This paper presents the HFB-PPT concept and preliminary results.

1. Introduction

The Pulsed Plasma Thruster (PPT) was the first electric thruster to be used in space, in 1964, with the Soviet space probe Zond 2. In the USA, the first PPT was used in the LES-6 satellite, launched in 1968. Other electric thrusters, such as the augmented hydrazine thrusters, arcjets, ion and Hall thrusters were developed later (Burton and Turchi, 1998).

Pulsed plasma thrusters are electric thrusters that allow very precise maneuvers and present relatively simple construction, high reliability, low cost and long lifetime. They can be used in satellites, space probes and other spacecrafts for orbit control and maintenance (LaRocca, 1966, Guman and Nathanson, 1970; Vondra et al., 1971, Vondra and Thomassen, 1971, 1974; Vondra, 1976), orbit transfer (Akimov et al, 1997), drag compensation and flight formation (Ebert et al, 1989; Janson, 1993) and attitude control (Meckel et al, 1997).

In the PPT the impulse is derived from an electric discharge applied on the surface of a solid dielectric, in general Teflon™ (PTFE – Polytetrafluoroethylene), causing its sublimation, dissociation and ionization. The generated plasma is then accelerated by the

Lorentz force which results from the coupling of the electric current and the self-induced magnetic field (Burton and Turchi, 1998). A parcel of the sublimated propellant is not ionized, being accelerated only by thermal expansion (Vondra et al., 1970), this portion is also known as late time ablation (LTA).

The High Frequency Burst Pulsed Plasma Thruster (HFB-PPT) was designed specifically to minimize the effects of the LTA. It is, therefore, convenient to give further details about the LTA.

Late time ablation is the sublimation of the propellant that takes place after a pulse discharge and happens because the propellant surface remains hot after the main discharge, above the sublimation temperature. This causes a significant part of the propellant (~40% in some cases) to be ejected at very low speeds, compared to the speeds of electromagnetically accelerated propellant. This low speed material does not contribute significantly to the impulse generated by the PPT and therefore current PPTs use approximately only 60% of the propellant to produce usable thrust.

In order to minimize the LTA problem a new PPT design was conceived. The approach to solve this problem was to try to electromagnetically accelerate the LTA by employing an additional pulse (or pulses) after the main discharge occurs. However, if these additional pulses were to happen in the same set of electrodes, near the propellant surface, the propellant would receive more heat which would lead to more LTA. Therefore, the additional discharges should take place downstream, relatively far from the surface, in a separate set of electrodes. It was clear also that a synchronization system had to be used to allow the secondary pulses to occur only after the main discharge occurred. Also, it was desirable to have a switch system capable of triggering several pulses in the extra pair of electrodes in order to investigate the effects of the timing and different pulse patterns in the performance of the HFB-PPT. Figure 1 shows the HFB-PPT discharge chamber.

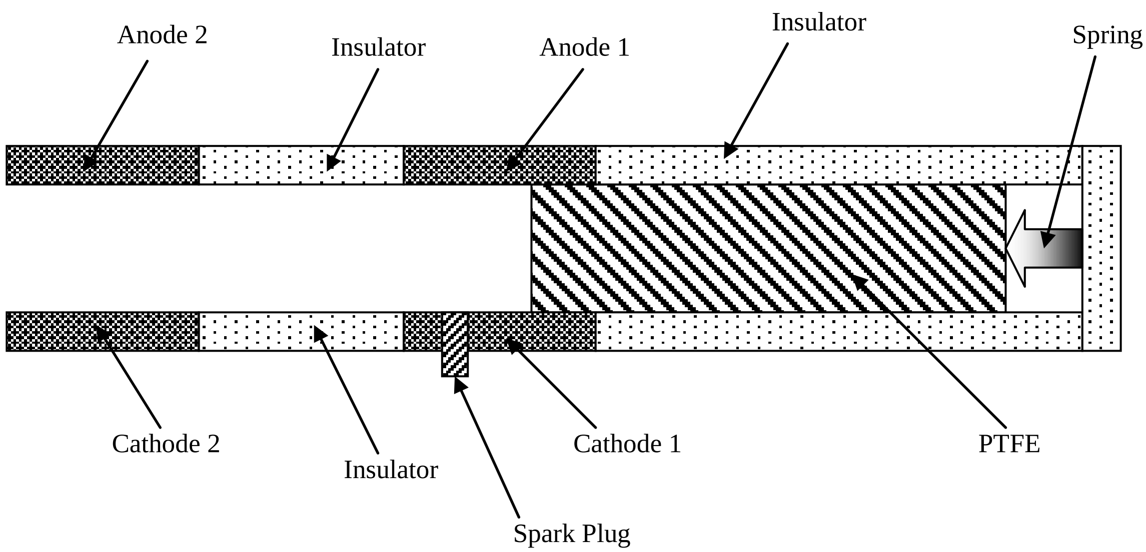

Figure 1 – HFB-PPT Discharge Chamber.

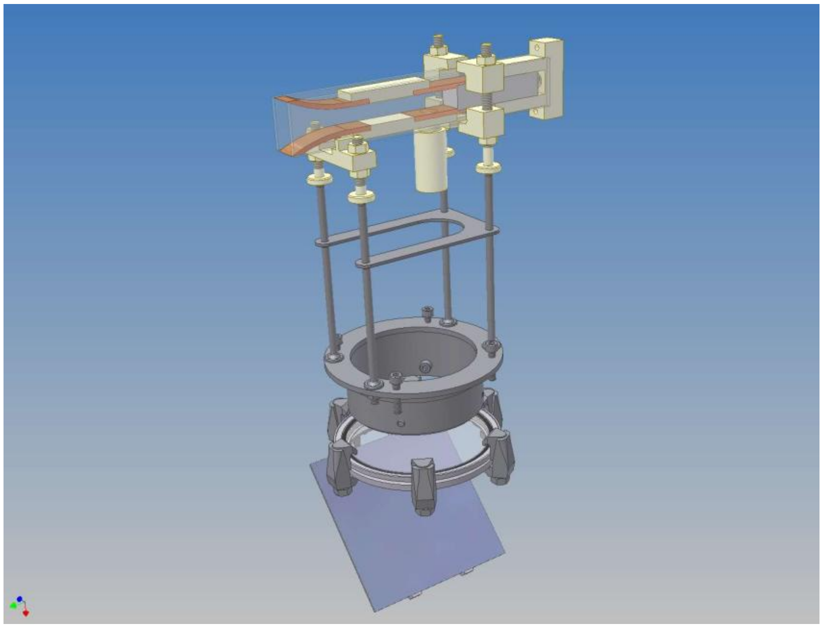

Figure 2 - The model of the developed HFB-PPT (top) mounted on its support (center) with a mirror on the bottom for instrumentation purposes.

Figure 2 shows the computer model of our developed prototype of HFB-PPT with its interface, allowing the thruster to be mounted horizontally or vertically, depending on the type of diagnostics desired. In this prototype the second set of electrodes also acts as divergent nozzle. For diagnostic reasons the prototype was assembled with glass on both sides. A spark plug is also present, close to the first set of electrodes.

2. HFB-PPT Control System

An open loop control system was chosen as a first approach to control the discharges. As this was a laboratory prototype it was our intention to make the control circuit as flexible as possible. Therefore, it was used a small flight computer running a proprietary operating system and a developed software in ‘C’ language. This system would allow us to program detailed discharge bursts to investigate the impact on efficiency. Figure 3 shows a block diagram of the HFB-PPT with the digital control unit. In this configuration three switches are employed to control the discharge of three capacitors.

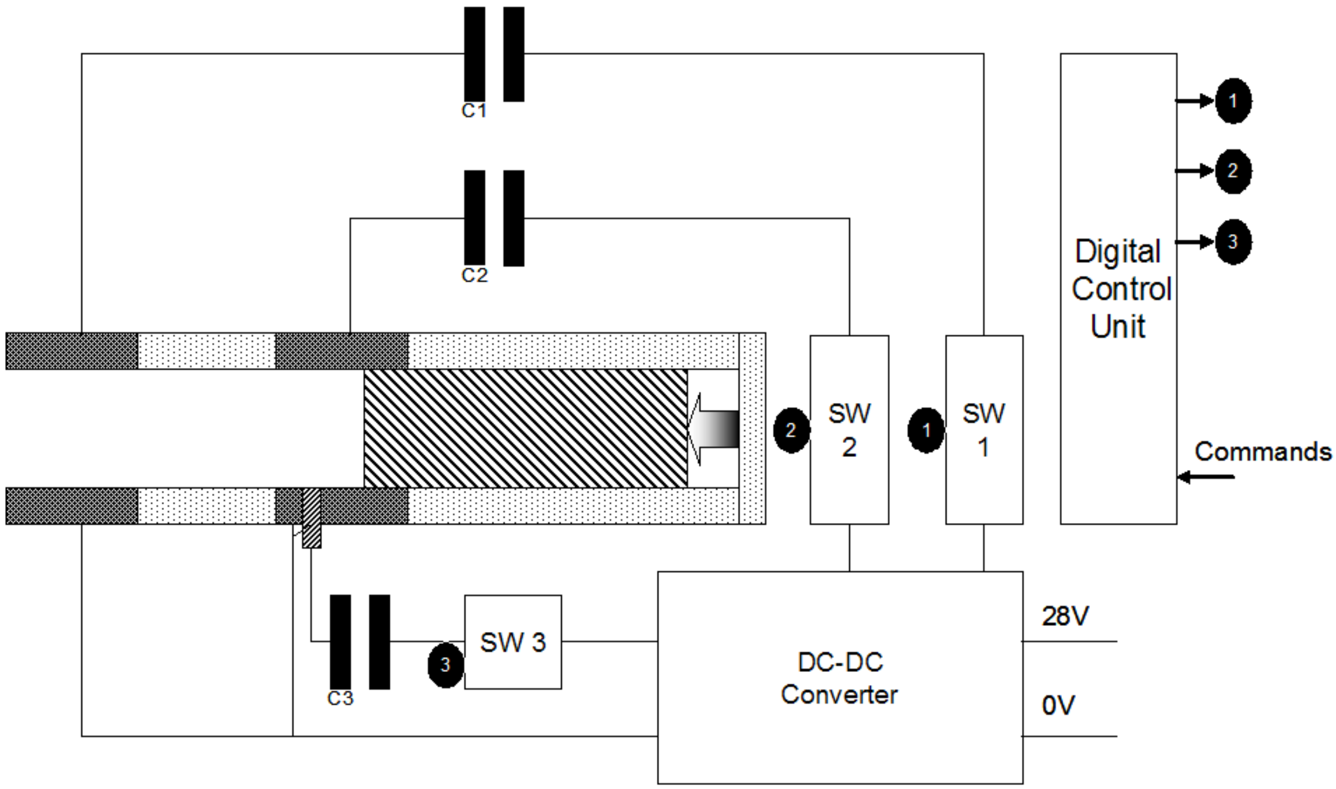

Figure 3 – A block diagram of the HFB-PPT.

3. A typical cycle of the HFB-PPT

At the beginning of the cycle all capacitors are charged with its nominal voltages. The Digital Control Unit (DCU) sends a command signal to the switch number three SW3, which controls the capacitor number three C3, the spark plug capacitor. The DCU also sends a signal to SW2 to let the capacitor C2 discharge, after the spark plug ignited. Thus a regular PPT cycle is finished. The novelty of the HFB-PPT starts from this point on. After a predetermined amount of time, with the intention of accelerating the LTA, the switch SW1 receives ON/OFF signals. These signals can be either only one single ON signal or a burst of ON/OFF signals with different time intervals between them or at a fixed frequency – this frequency can reach ~1 MHz hence the name of the thruster.

Based on the cycle above, some of the switches may seem unnecessary at first, like the SW2. However, since this is a development platform, the SW2 can be used when the voltage applied on capacitor C2 is greater than the breakdown voltage for the main discharge's electrodes. In this case the spark plug circuit would not be used for the main discharge. But there is the possibility of triggering the spark plug after the main discharge to help the LTA being accelerated by the second pair of electrodes downstream.

4. Test Facilities

The HFB-PPT was tested in the Astronautics Research Group (ARG) laboratories in the University of Southampton in England. The vacuum chamber was cylindrical and was 1.2 m long and 0.8 m diameter. It was used a rotary pump and a cryogenic pump. All tests were carried out at pressures of less than 5×10^{-6} mbar. Electric currents were measured using Rogowski coils and a digital oscilloscope. Voltages were measure using high voltage probes (1000:1) and standard voltage probes connected to a digital oscilloscope. Images were obtained using a digital camera.

5. Preliminary Tests and Results

The tests presented here are part of the first phase of characterization of the HFB-PPT. It was used a 110 μF capacitor for the main discharge and a 4700μF capacitor for the secondary discharge. The high capacitance of the secondary discharge was chosen to investigate maximum lengths of secondary discharges. In this phase the HFB-PPT was tested with three different main discharge voltages (1 kV, 1.5 kV and 2 kV) and fourteen different secondary discharge voltages (0, 3.75, 7.5, 15, 30 35, 50, 75, 100, 150, 200, 250, and 300 V). A single second pulse was employed in all cases and there was no added delay between the first pulse and the second pulse. The intention with these tests was to observe how the currents and voltages of the secondary discharge behave with single pulse and *zero* delay in the DCU to serve as a base for the next tests. The low voltages applied to the secondary discharges were used to investigate the time of flight and the effects of the first discharge on the secondary discharge. In this mode the HFB-PPT operates like a two-stage solid pulsed plasma thruster.

It was observed four distinct regimens during the tests. The regimens are delimited by increasing the second discharge voltage.

The first regimen, shown in Fig. 4, occurs at very low voltage (0 to 50 V, depending on the main discharge voltage), has an oscillatory secondary discharge current 90^o out of phase with relation to the main discharge. The length of the discharge is approximately the same as the main discharge. A current was measured even when the secondary capacitor was initially discharged and there was a residual voltage in the secondary capacitor, directly proportional to the main discharge voltage. The analysis of this phenomenon is out of the scope of this paper, but will be investigated in the future as a possible diagnostic tool for the HFB-PPT or other plasma thruster.

The second regimen, shown in Fig. 5., at an intermediate voltage (between 30 and 75 V, depending on the main discharge voltage) and shows a mainly positive current for the secondary discharge, still out of phase, although not exactly 90^o. The length of the discharge is longer than the first regimen, with a long tail after the main discharge is over.

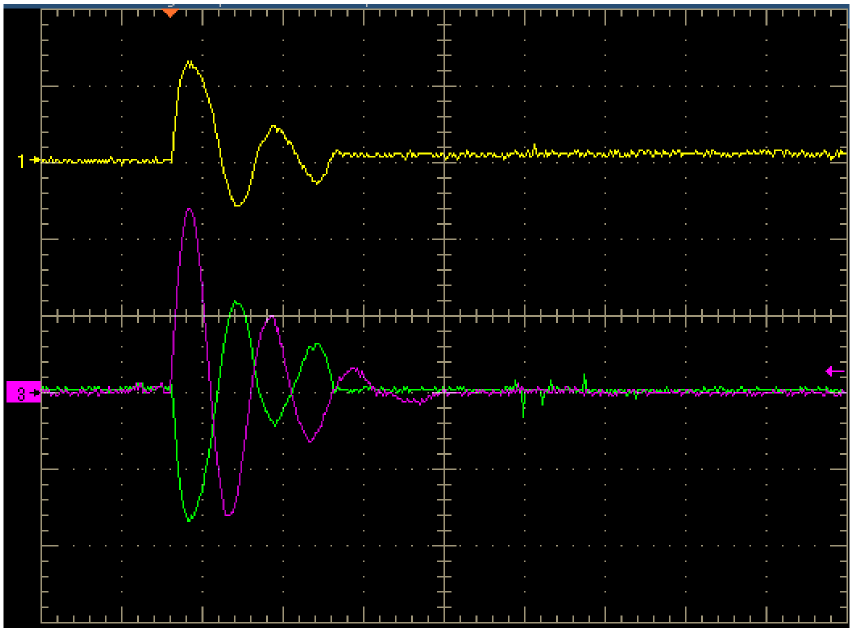

Figure 4. – First regimen. Typical discharge for secondary discharge voltages between 0 and 50V (with primary discharge voltage of 1 kV or 1.5 kV) and between 0 and 15 V (with primary discharge voltage of 2 kV), showing the secondary discharge capacitor voltage (yellow, 100V/div), secondary discharge current (green, 500 A/div) and primary discharge current (pink, 2000 A/div) at 100 μs/div (horizontally). Taken with 2 kV primary discharge and 0 V secondary discharge.

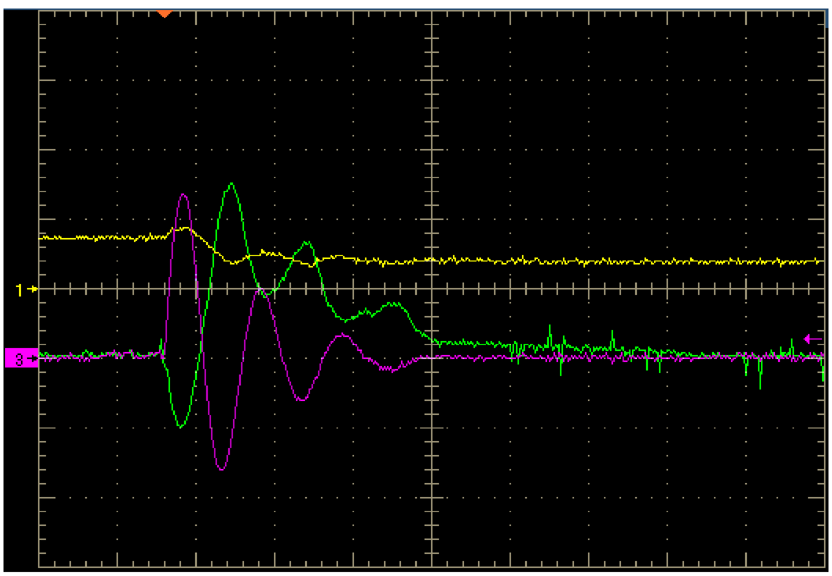

Figure 5. – Second regimen. Typical discharge for secondary discharge voltage of 50V (with primary discharge voltage of 1.5 kV) and between 30 and 75 V (with primary discharge voltage of 2 kV) – not observed at 1 kV-, showing the secondary discharge capacitor voltage (yellow, 100V/div), secondary discharge current (green, 500 A/div) and primary discharge current (pink, 5000 A/div) at 100 μs/div (horizontally). Taken with 2kV primary discharge and 75 V secondary discharge.

The third regimen, shown in Fig.6, is similar to the second regimen but has a more pronounced tail and is in the transition to the fourth regimen. There are two observable phases, an oscillating phase that lasts while the main discharge occurs and a second phase that resembles a critically dumped circuit.
The fourth regimen, shown in Fig. 7, has a completely positive second discharge current and resembles the current shape of a critically damped circuit, although it also has a not so pronounced oscillating phase during the main discharge. The length of the discharge is much longer than the main discharge.

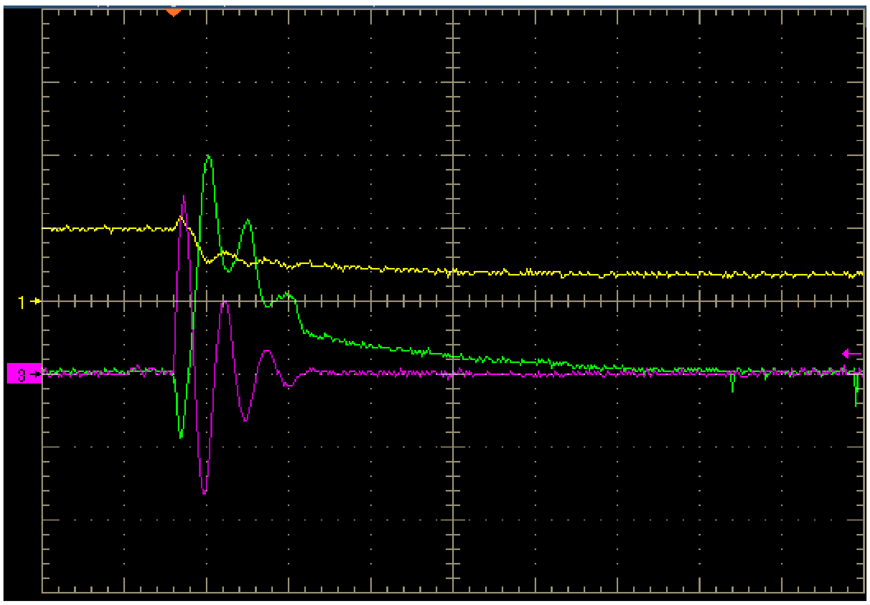

Figure 6. – Third regimen. Typical discharge for secondary discharge voltage between 75 V and 100V (for all three primary voltages), showing the secondary discharge capacitor voltage (yellow, 100V/div), secondary discharge current (green, 500 A/div) and primary discharge current (pink, 5000 A/div) at 100 µs/div (horizontally). Taken with 2kV primary discharge and 100 V secondary discharge.

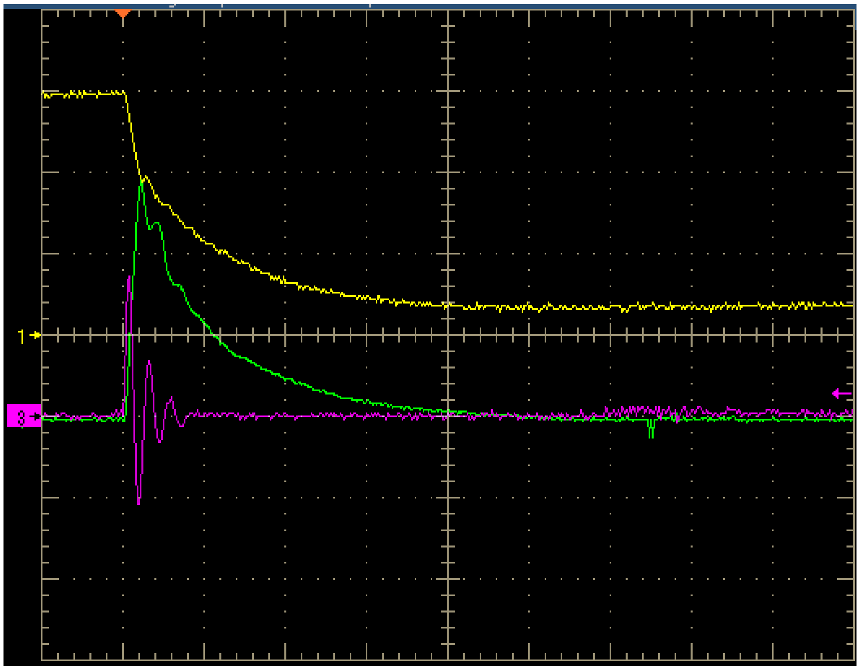

Figure 7. – Fourth regimen. Typical discharge for secondary discharge voltages above 150 V (for 1 kV main discharge), 200 V (for 1.5 kV main discharge) or 250 V (for 2 kV main discharge), showing the secondary discharge capacitor voltage (yellow, 100V/div), secondary discharge current (green, 1000 A/div) and primary discharge current (pink, 5000 A/div) at 100 µs/div (horizontally). Taken with 1.5kV primary discharge and 300 V secondary discharge.

Measurements of the second discharge to investigate its length, delay with respect to the first discharge, and maximum current were carried out. Figure 8 shows the length of the discharges for all the fourteen voltages of the second discharge at three different main discharge voltages. It can be seen an abrupt change in the length of the discharge at around 75 V and a tendency of an increasing length. For comparison, the main discharge length is also plotted.

Figure 9 shows the measured delays between the first and second discharge. There is a maximum delay observed at different points, depending on the main discharge voltage. For 1 kV main discharge there is a maximum at 150 V second discharge. For 1.5 kV main discharge the maximum is at 200 V and for 2 kV the maximum is at 250 V.

The maximum currents for the second discharge were measure, shown in Fig. 10, and are observed to be directly proportional to the second discharge voltage in a linear fashion, with the angular coefficient proportional to the main discharge voltage. It can be seen that even when the second discharge capacitor has 0 V there is a considerable current flowing. This minimum current is proportional to the main discharge voltage.

Figure 11 shows a picture of the HFB-PPT firing. This picture is an integral of the primary and secondary shots and was taken with 1.5 kV main discharge, 200 V secondary discharge.

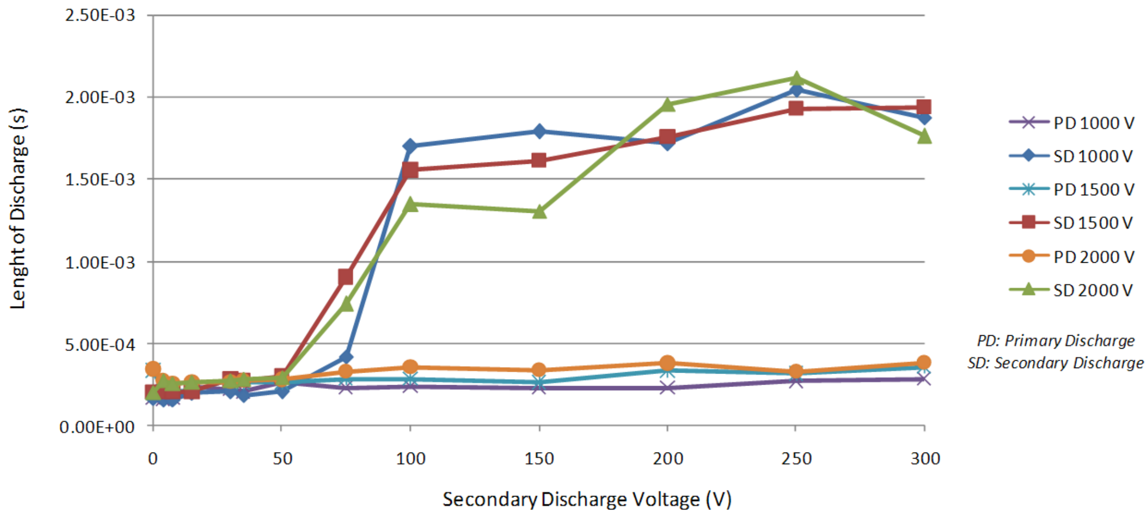

Figure 8. - Length of the secondary discharge as a function of the voltage applied in the secondary electrodes for three different primary discharge voltages.

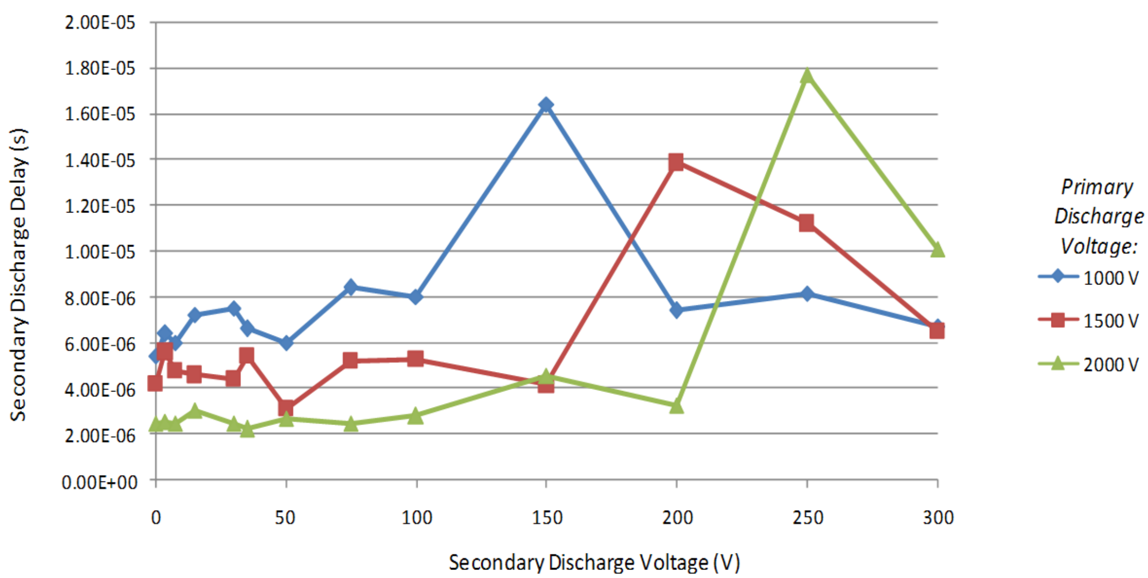

Figure 9. – Delay between the first discharge and the second discharge as a function of the voltage applied to the secondary electrodes for three different primary discharge voltages.

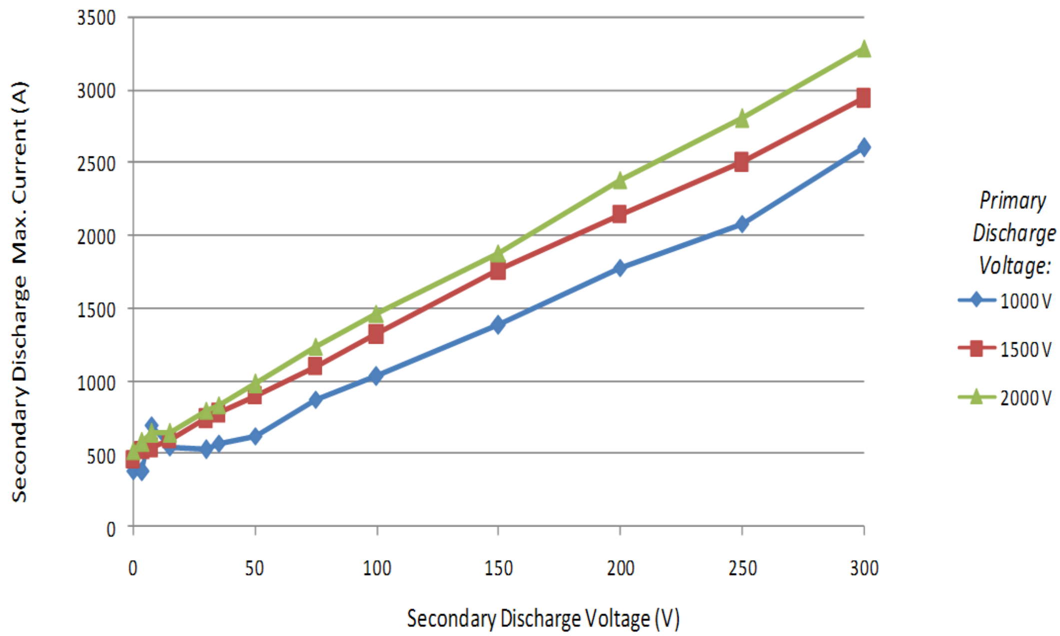

Figure 10. – Maximum Current in the secondary discharge as a function of the secondary discharge voltage for three different primary discharge voltages.

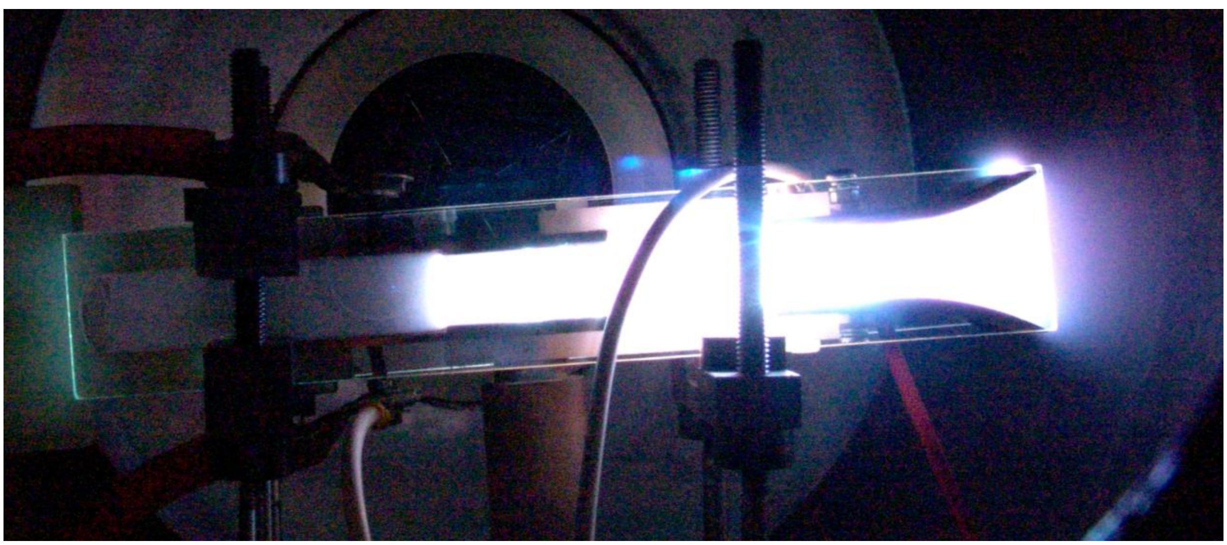

Figure 11. – HFB-PPT firing.

6. Discussion and Conclusion

The first regimen of the secondary discharge is largely dependent on the main discharge that, in fact, generates current between the secondary electrodes even when its capacitor is completely discharged.
The second regimen shows an oscillatory discharge with an offset, given by the increased voltage in the secondary discharge. A critically dumped discharge is observed after the

end of the main discharge, although not very pronounced. The third regimen shows a more pronounced critically dumped phase after the main discharge ended and the fourth regimen shows an even more pronounced critically dumped behavior.
After the main discharge is over, there is no more plasma being produced upstream and the propellant starts to produce the LTA. As a first hypothesis, the current flowing in the secondary electrodes, at this point, would supposedly be flowing in the LTA. A more in-depth analysis will be carried out to validate this hypothesis.
Tests measuring the length of the discharge showed an increasing length of discharge with the second discharge voltage, but also indicates that, for a given main discharge voltage, there is a maximum length of the secondary discharge. This characteristic supports the hypothesis that the secondary current discharge would be flowing on the LTA, as there is a limited amount of LTA for a given main discharge voltage. In fact, a residual voltage was measured in the secondary capacitor for secondary discharge voltages above 200 V.
The maximum delays observed at different secondary discharge voltages indicate that the transition of the secondary discharge from an oscillatory mode, with the first part negative, to a completely positive discharge occurs at different voltages, depending on the main discharge voltage. As it can be observed when there is 0 V applied on the secondary capacitor, a current on the secondary electrodes is generated by the main discharge with the first bit negative. To overcome this first negative bit and initiate the positive only discharge current it is necessary to have increasingly more voltage on the secondary capacitor as the main discharge voltage is increased. These voltages can be seen as the voltages above which the discharge is completely positive. A finer change in the secondary discharge voltages is required to analyze exactly where the peak occurs and the behavior its vicinity.

7. Acknowledgments

The first author acknowledges CNPq – Conselho Nacional de Desenvolvimento Científico e Tecnológico – part of the Ministry of Science and Technology of Brazil, for granting a PhD scholarship.

References

Burton, R.L., Turchi, R.J., 1998, “Pulsed Plasma Thruster”, Journal of Propulsion and Power, Vol.14, No.5.

LaRocca, A.V., 1966, “Solid Propellant Electrical Thrustors for Attitude Control and Drift Correction of Space Vehicles”. In 5th Electric Propulsion Conference, San Diego, California, March 7-9, AIAA Paper 66-229.

Guman, W.J., Nathanson, D.M., 1970, “Pulsed Plasma Microthruster Propulsion System for Syncronous Orbit Satellite”, Journal of Spacecraft, Vol. 7, No. 4.

Vondra, R.J., Thomassen, K.I., Solbes, A., 1970, ”Analysis of Solid Teflon Pulsed Plasma Thrusters”, Journal of Spacecraft and Rockets, Vol.7, No.12, August, pp. 1402-1406.

Vondra, R.K., Thomassen,K., and Solbes, A., 1971, “A Pulsed Electric Thruster for Satellite Control”, Proceedings of the IEEE, Vol. 59, No.2, pp. 271-277.

Vondra, R.J., Thomassen, K.I., 1971, ”Exhaust Velocity Studies of a Solid Teflon Pulsed Plasma Thruster.” Journal of Spacecraft and Rockets Vol.9. No.1. August, pp. 61-64.

Vondra, R.J., Thomassen, K.I., 1974, ”Flight Qualified Pulsed Electric Thruster for Satellite Control.” Journal of Spacecraft and Rockets, Vol.11, No.9, September, pp. 613-617.

Vondra, R.J., 1976, “The MIT Lincoln Laboratory Pulsed Plasma Thruster-A Final Report on the LES-8/9 Pulsed Plasma Thruster”, AIAA Paper 76-998.

Akimov, V., Nagel, I., Ogloblina, I., Antropov, N., Pokryshkin, A., Popov, G., Rudikov, A., 1997, “Analysis of PPT Potentialities in Solving the Sattellite Orbit Control Tasks”, 25^{th} International Electrical Propulsion Conference, Paper IEPC-97-146.

Ebert, W.L., Kowal, S.J., Sloan, R.F., 1989, “Operational Nova Spacecraft Teflon Pulsed Plasma Thruster System”, ASME, SAE and ASEE, 25th Joint Propulsion Conference, AIAA Paper 89-2497.

Janson, S.W., 1993, "The On-Orbit Role of Electric Propulsion", AIAA Paper 93-2220.

Meckel, N. J., Cassady, R.J., Osborne, R. D., Hoskins, W.A., Myers, R. M., 1997, “Investigation of Pulsed Plasma Thrusters for Spacecraft Attitude Control”, IEPC-Paper 97-128, Cleveland, OH, USA.